nature plants
SUPPLEMENTARY INFORMATION
VOLUME: 3 | ARTICLE NUMBER: 16193
In the format provided by the authors and unedited.

Simulating US agriculture in a modern Dust Bowl drought

Michael Glotter[1†]* and Joshua Elliott[2,3†]

[1]Department of the Geophysical Sciences, University of Chicago, 5734 S Ellis Ave, Chicago, Illinois, 60637, USA. [2]NASA Goddard Institute for Space Studies, 2880 Broadway, New York, New York 10025, USA. [3]Computation Institute, University of Chicago, 5735 S Ellis Ave, Chicago, Illinois 60637, USA. [†]These authors contributed equally to this work. *e-mail: glotter@uchicago.edu

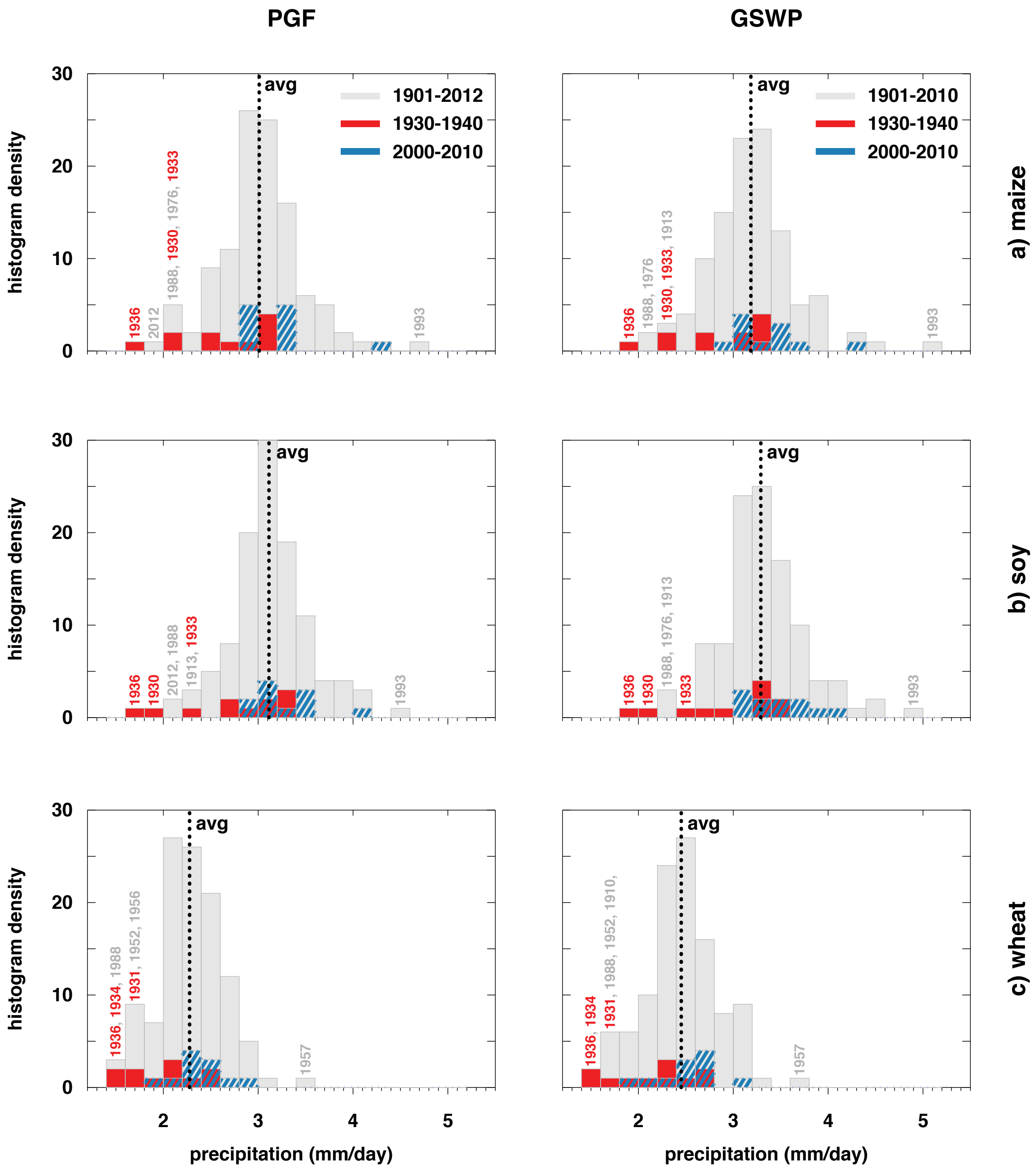

Supplementary Figure 1: Histogram of historical PGF (left) and GSWP (right) precipitation weighted by present-day U.S. a) maize, b) soy, and c) wheat production. Data are averaged over months JJA (June, July, August) for maize and soy, and AMJ (April, May, June) for wheat. PGF data span years 1901-2012, and GSWP years 1901-2010. The six driest and single wettest years are identified in text (ordered by rainfall amounts within bin, with the lowest amount at the bottom). The 1930s (red) includes three out of the six driest seasons for all crops.

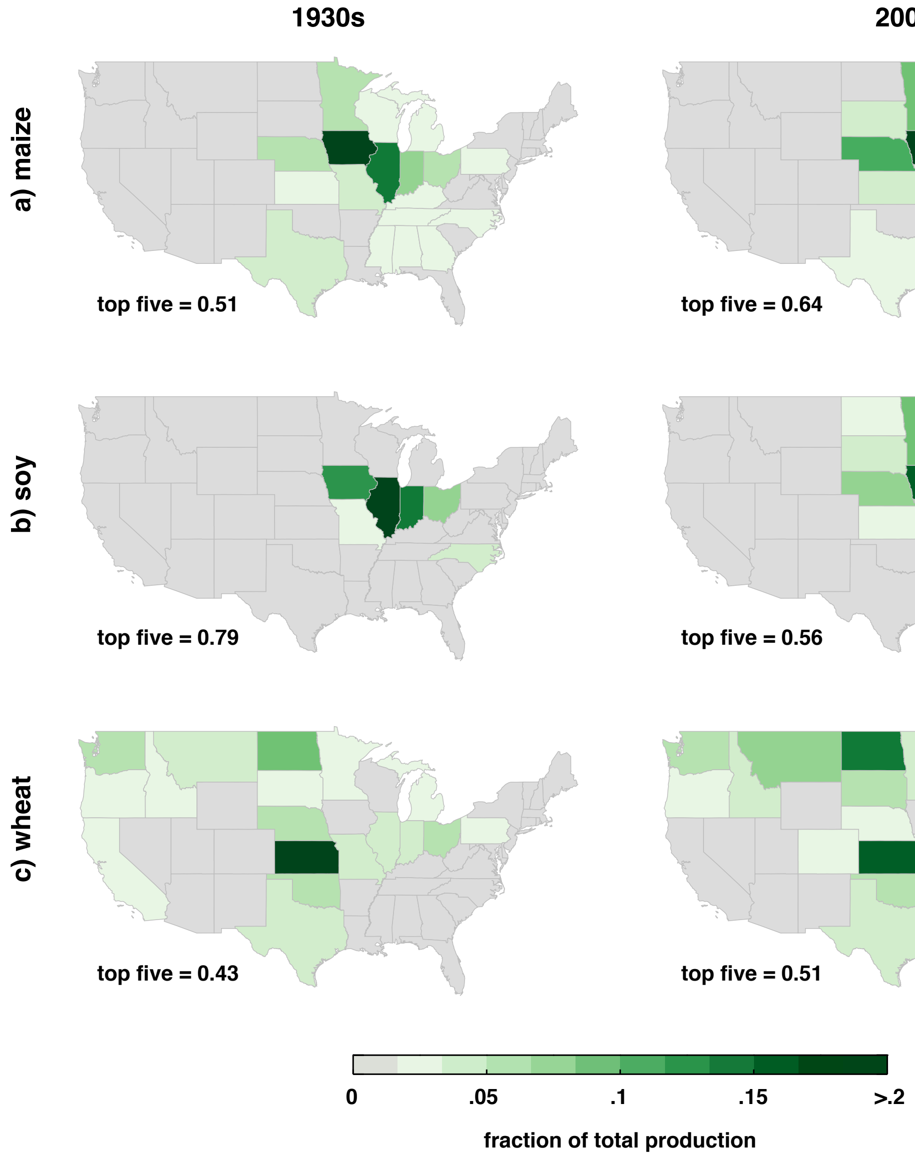

Supplementary Figure 2: Fraction of 1930-1940 (left) and 2000-2010 (right) U.S. a) maize, b) soy, and c) wheat production by state. For each crop, the fraction of production from the top five producing states in the 2000s is marked in text. The 2000s maize and soy top five producing states are concentrated in the upper Midwest in Illinois, Indiana, Iowa, Minnesota, and Nebraska. The 2000s wheat top five producing states are scattered in the West in Kansas, Montana, North Dakota, Oklahoma, and Washington.

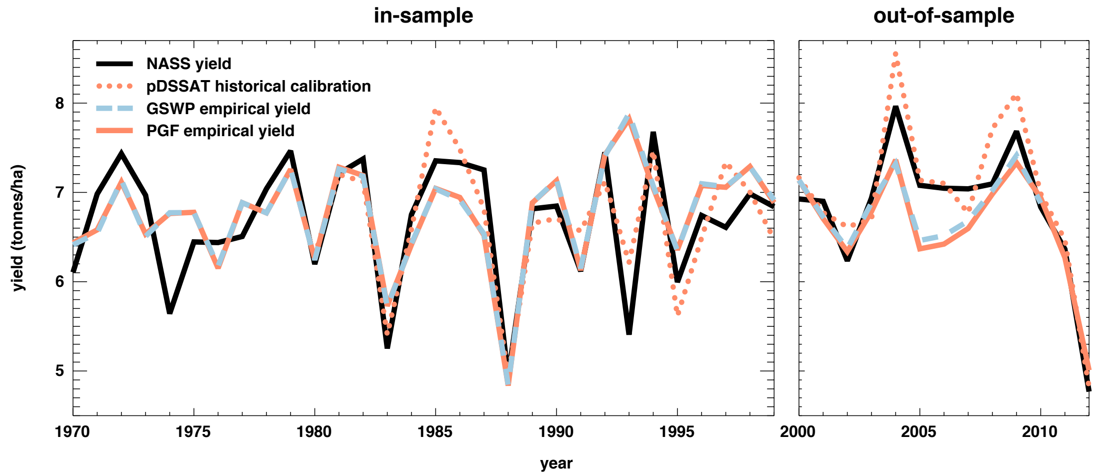

Supplementary Figure 3: 1970-2012 observed (black) and empirically estimated national maize yields. GSWP (red solid) and PGF (blue dashed) empirical models are calibrated over years 1970-1999 (left), and projected out-of-sample to 2010 for GSWP and 2012 for PGF (right). Estimated 1980-2012 process-based model yields from the pDSSAT historical calibration are shown for comparison (red dotted). We detrend observed and pDSSAT yields to compare to empirical models that do not include technological advancements. (Yield anomalies are sensitive to detrending method, especially at the endpoints, so comparison of observations and simulations with trends is preferred [Fig. 8, top panel]. See Methods for discussion.) The empirical models successfully capture patterns in yield loss from large-scale drought, but underestimate the extent of such loss. This empirical design cannot capture yield loss from frost and flood in 1974 and 1993, respectively.

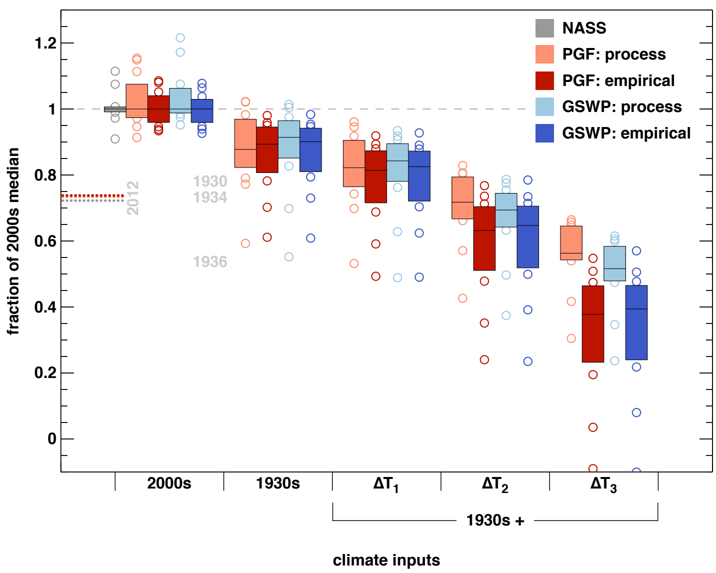

Supplementary Figure 4: Box plots of U.S. maize yields for process (light) and empirical (dark) models driven by both PGF (red) and GSWP (blue) climate sources. Boxes represent national yields within the interquartile range (i.e., the 25^{th} and 75^{th} percentiles), and circles represent yields outside of this range. Process model simulations assume 2012 CO_2 and technology. NASS observed yields for the 2000s are detrended using a 1980-2015 trendline, and shown in gray. Dotted lines represent 2012 yields. Yields estimated from process and empirical models are similar, but empirical simulations become unphysical for the most severe scenarios, far outside calibrated conditions.

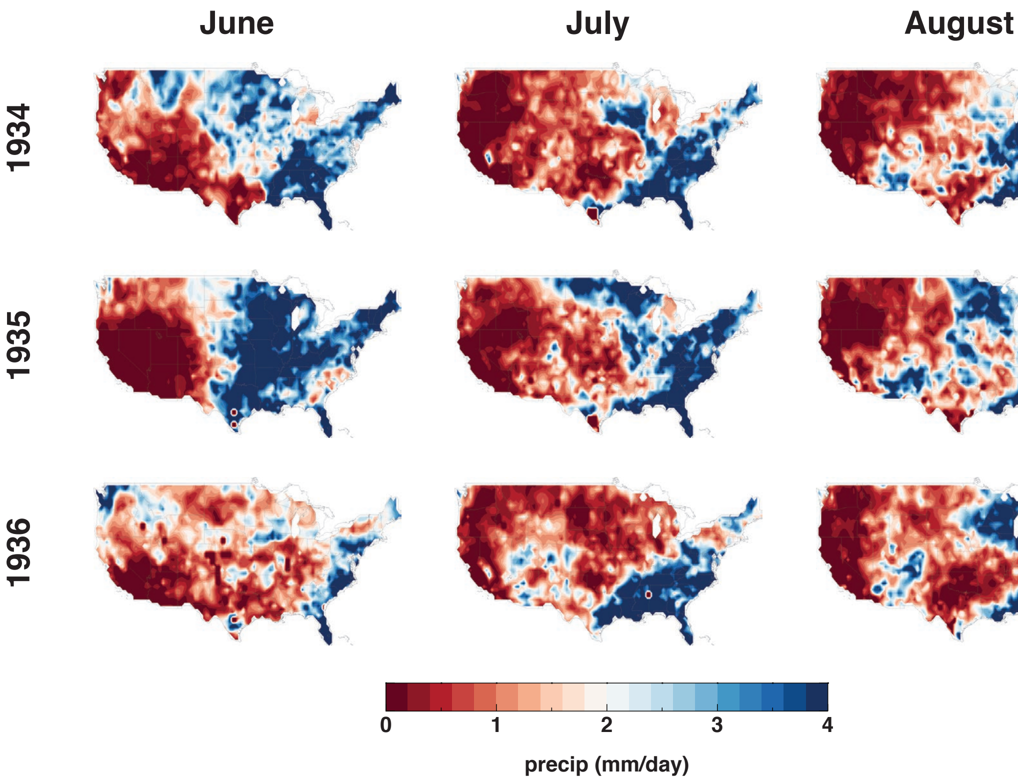

Supplementary Figure 5: Maps of monthly average PGF precipitation for years 1934-1936. The drought in 1934 was primarily concentrated in the western U.S., covering most wheat-growing regions. Key maize- and soy-growing regions in the corn belt, however, were uniquely saved by heavy precipitation in the most critical month in July. The drought of 1936 was more widespread across the U.S. For comparison, we show precipitation in 1935. Growing season precipitation—especially in the corn belt—was more typical in 1935 than 1934 and 1936.

Supplementary Table 1: Shifts in maximum temperatures from years 1920-1939 to 1980-2009 (ΔT_1), 2010-2039 (ΔT_2), and 2040-2069 (ΔT_3). We shift 1930s climate using GCM-estimated changes in 30-year average monthly climate. (See Methods.) Here, temperature shifts are averaged by season (JJA for maize and soy, and AMJ for wheat) and weighted by crop production for illustrative purposes only.

	seasonal tmax shift (°C)		
	ΔT_1	ΔT_2	ΔT_3
maize	0.8	2.3	3.8
soy	0.8	2.2	3.8
wheat	0.4	1.7	3.2

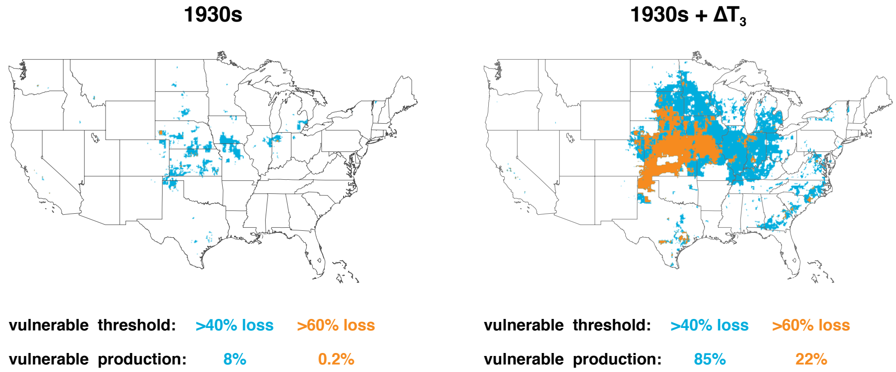

Supplementary Figure 6: Locations where successive droughts may have lasting impacts on rainfed maize production. Estimates in left panel use 1930s weather and 2012 CO_2/technology, and estimates in right panel use $1930s + \Delta T_3$ weather (1930s weather with temperature shifted to 2040-2069 averages) and 2035 CO_2/technology. Colored areas mark grid cells where 1933-1937 mean rainfed yield losses are more than 40% (blue) or 60% (orange) of 2000s median rainfed yields. Annual yields <1 tonne/ha are assumed to be left unharvested (i.e., yield=0). 1930s simulations estimate <10% of production vulnerable to consecutive droughts, but high warming simulations estimate >20% vulnerable to consecutive droughts.

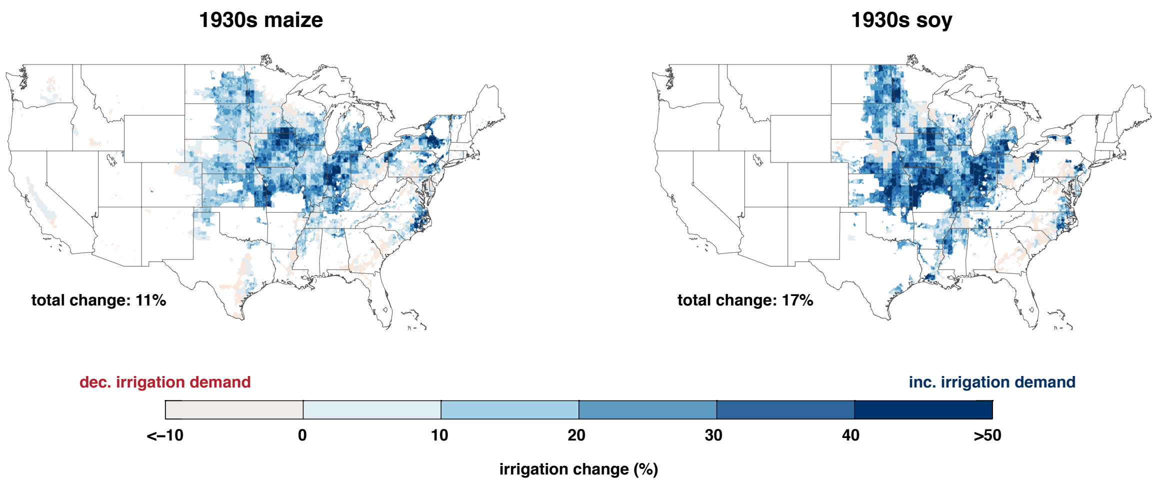

Supplementary Figure 7: Irrigation demand change from 2000s median to 1933-1937 mean for maize (left) and soy (right) yield simulations. Simulations use 2012 technology and PGF climate inputs, and estimate irrigation changes for only those areas irrigated in 2012. We do not estimate changes in water demand if currently rainfed fields are suddenly irrigated. 1933-1937 droughts increase U.S. irrigation demand ~11% for maize and ~17% for soy.

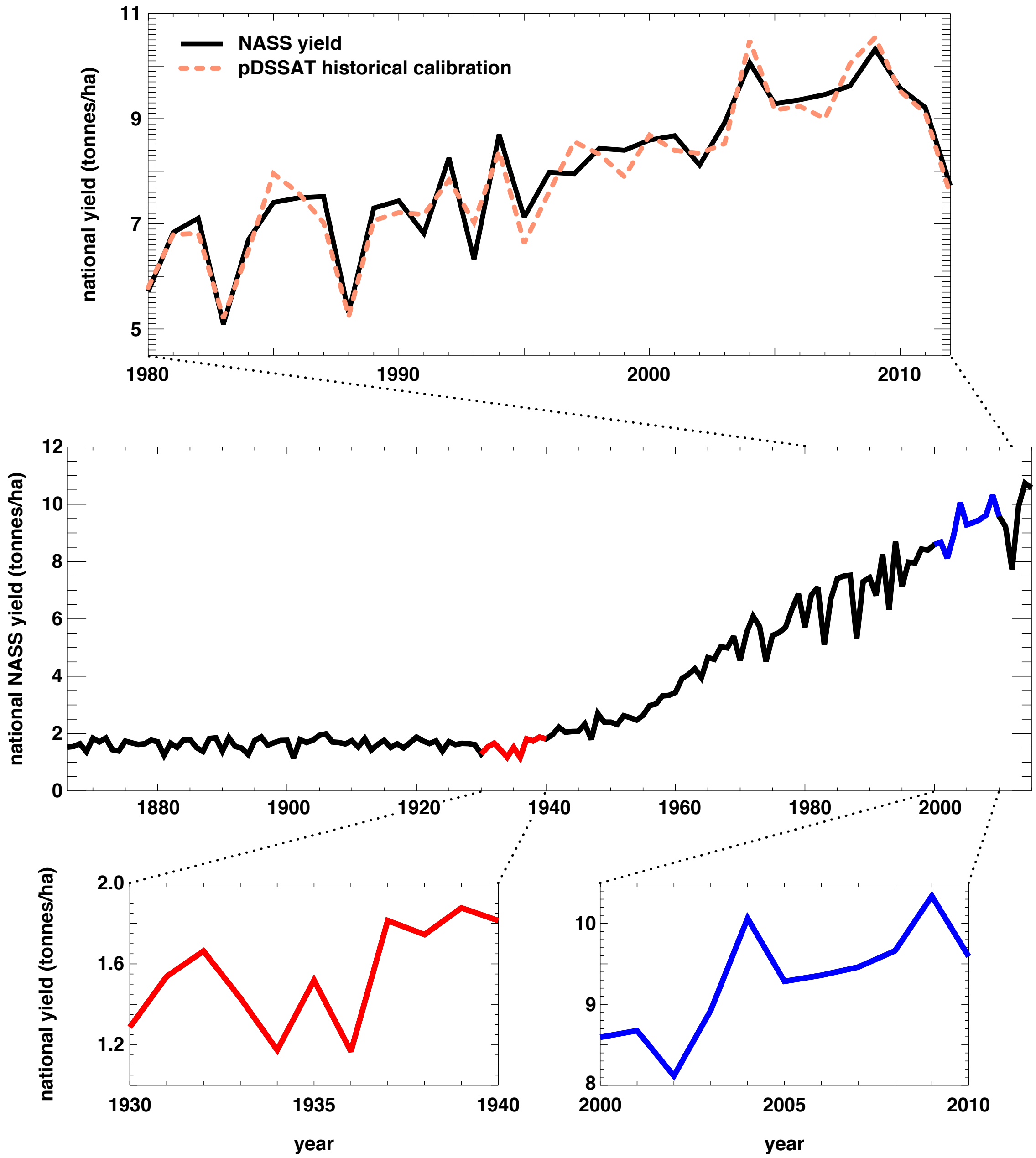

Supplementary Figure 8: 1866-2015 surveyed national NASS maize yields (middle panel). Yields from 1930-1940 and 2000-2010 are expanded for clarity (bottom panels). Changes in management and technology have improved yields by ∼5x from preindustrial to modern times, and process-based simulations successfully capture recent yield trends (top panel). Simulations of pDSSAT are calibrated using the Daymet climate dataset (native resolution of 1 km), reproducing observed national yields with a correlation coefficient of ∼0.97 (dashed orange). We model technological yield trends for validation purposes only, but use fixed technology around years 2012 and 2035 for the remainder of the manuscript.

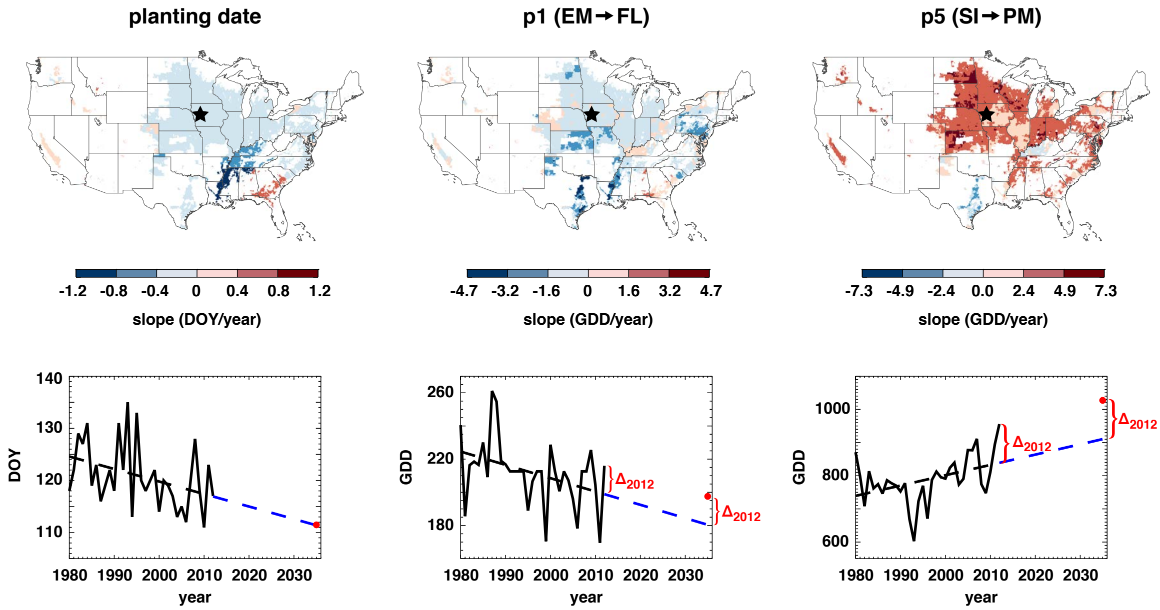

Supplementary Figure 9: Methodology for estimating technological advancements in future 2035 maize simulations. *top)* Slopes of linear trends in 1980-2010 maize planting date, p1 (growing degree days from emergence to flowering), and p5 (growing degree days from silking to physiological maturity). *bottom)* We estimate 2035 values (red dots) by extrapolating trends in planting date, p1, and p5 (dashed blue) and adding the deviations from trend in year 2012 (dashed red). Bottom panels demonstrate extrapolation for a sample location in Iowa, marked by stars in top panels.

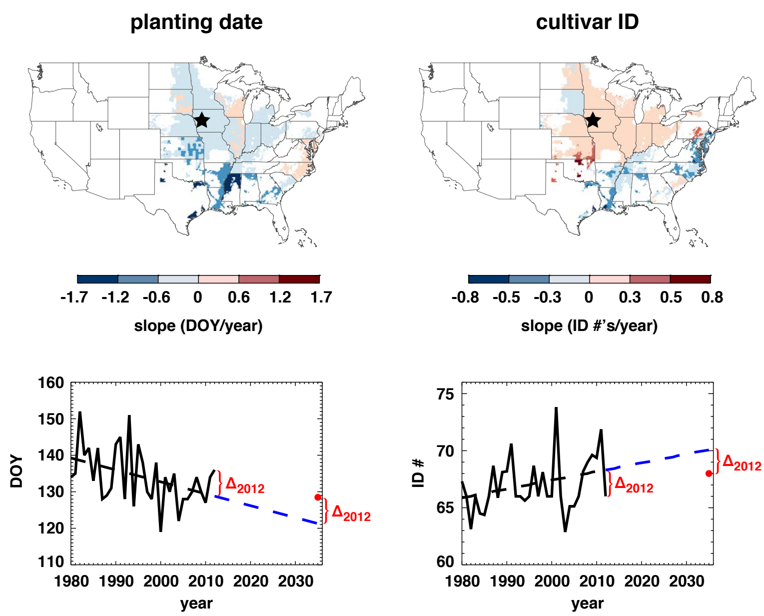

Supplementary Figure 10: Methodology for estimating technological advancements in future 2035 soy simulations. *top)* Slopes of linear trends in 1980-2010 soybean planting date and cultivar identification number. *bottom)* We estimate 2035 values (red dots) by extrapolating trends in planting date and cultivar identification (dashed blue) and adding the deviations from trend in year 2012 (dashed red). Bottom panels demonstrate extrapolation for a sample location in Iowa, marked by stars in top panels.

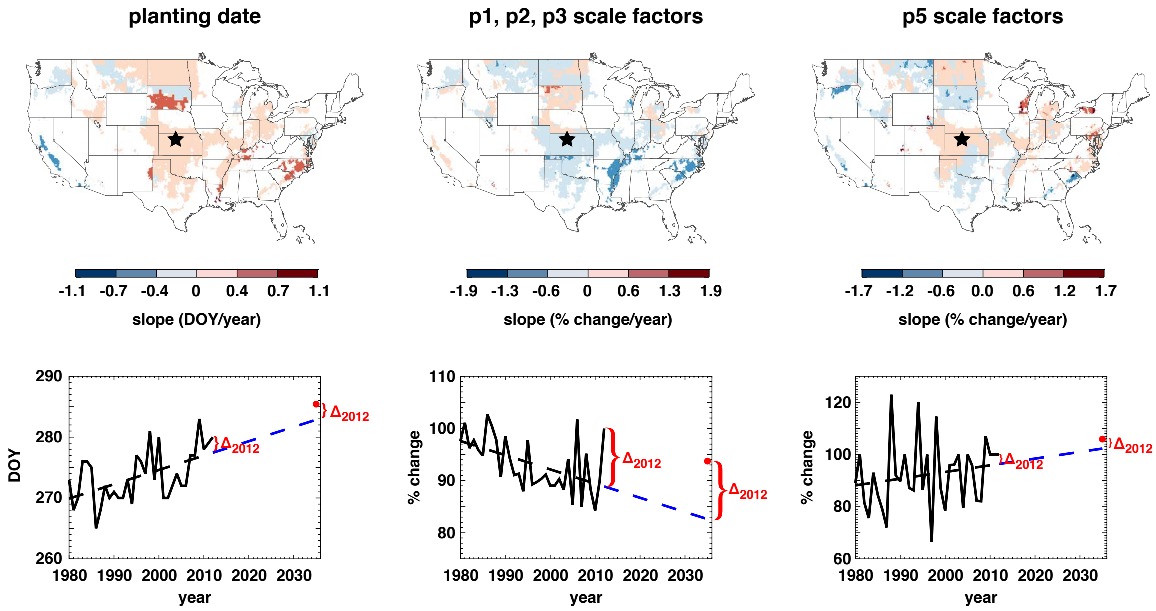

Supplementary Figure 11: Methodology for estimating technological advancements in future 2035 wheat simulations. *top)* Slopes of linear trends in 1980-2010 wheat planting date and scale factors for growth parameters $p1$ (flowering to terminal spikelet), $p2$ (terminal spikelet to end of leaf growth), $p3$ (end of leaf growth to end of spike growth), and $p5$ (grain filling duration). *bottom)* We estimate 2035 values (red dots) by extrapolating trends in planting date and growth parameter scale factors (dashed blue) and adding the deviations from trend in year 2012 (dashed red). Bottom panels demonstrate extrapolation for winter wheat at a sample location in northern Kansas, marked by stars in top panels.